Universal Nanosonosensitizer for ROS-Mediated reduction of various Cancer cells

Junna Jiao[1, 3], Kun Shao[4], Kaixin Wang[1, 3], Jiaxuan Liu[1, 3], Zhijie Weng[1, 3], Junrong Jiao[5*], Zhuangwei Lv[2, 3*]

1 School of Basic Medical Sciences, Xinxiang Medical University, Xinxiang, Henan, 453003, People's Republic of China

2 School of Forensic Medicine, Xinxiang Medical University, Xinxiang, Henan, 453003, People's Republic of China

3 Xinxiang Key Laboratory of Tumor Vaccine and Immunotherapy, School of Basic Medical Sciences, Xinxiang Medical University, Xinxiang, Henan 453003, People's Republic of China

4 Department of Pathology，Xinxiang Central Hospital，Henan Province，Xinxiang, Henan 453000, People's Republic of China

5 Key Lab for Special Functional Materials of Ministry of Education, School of Materials Science and Engineering; Henan University, Kaifeng 475004, People’s Republic of China

* Correspondence: Zhuangwei Lv, School of Forensic Medicine, Xinxiang Medical University, Xinxiang, Henan, 453003, People's Republic of China. Email: *201079@xxmu.edu.cn*

Junrong Jiao, Key Lab for Special Functional Materials of Ministry of Education, School of Materials Science and Engineering; Henan University, Kaifeng 475004, People’s Republic of China. Email: *jiaojr@vip.henu.edu.cn*

Supplementary Figures

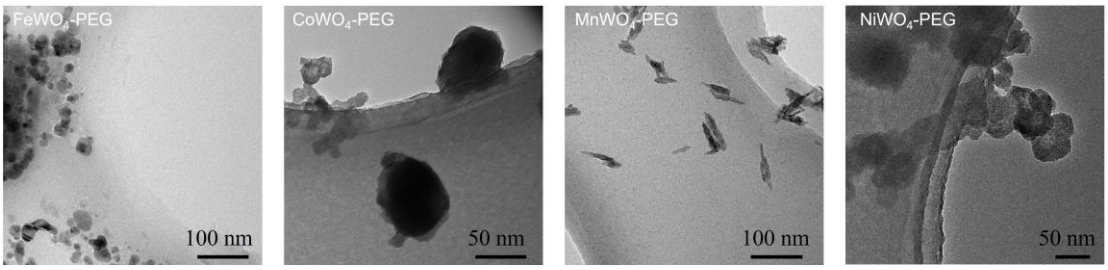

Figure S1 The TEM images of MWO_4-PEG (M= Mn Co Ni Fe) nanoparticles.

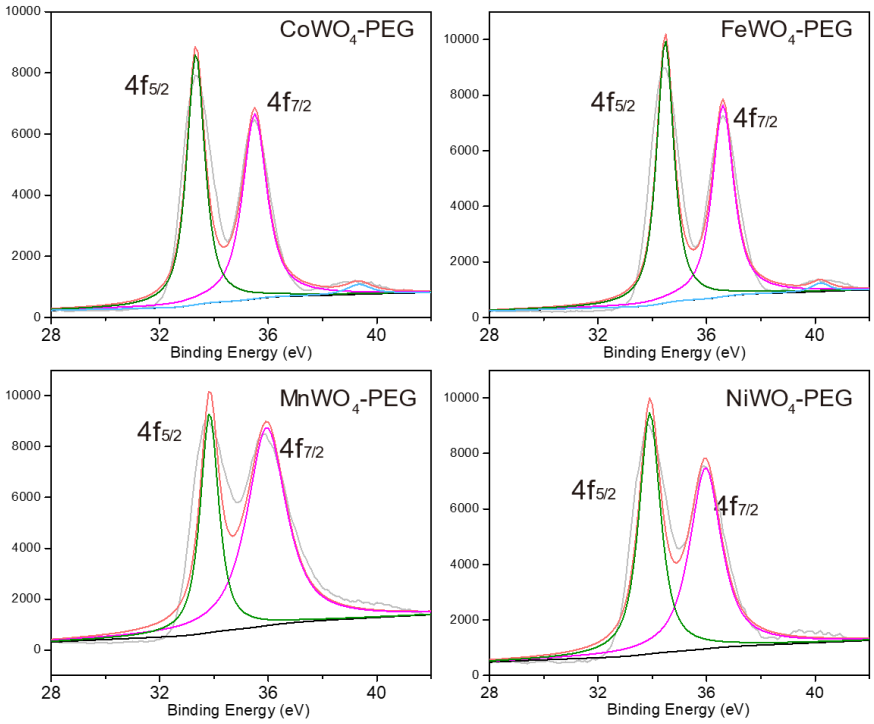

Figure S2 The XPS spectra of W 4f (K) peaks of MWO_4-PEG (M= Mn Co Ni Fe) nanoparticles.

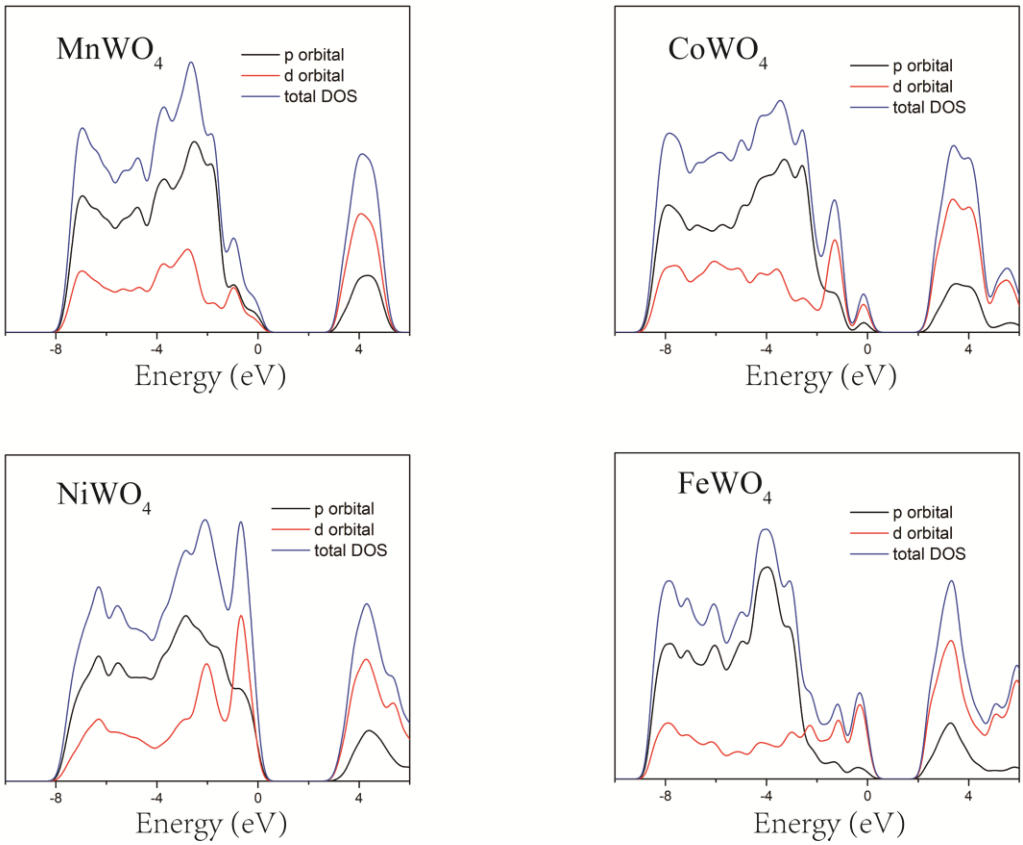

Figure S3 The total and partial density of states of MWO_4 (M= Mn Co Ni Fe) nanoparticles.

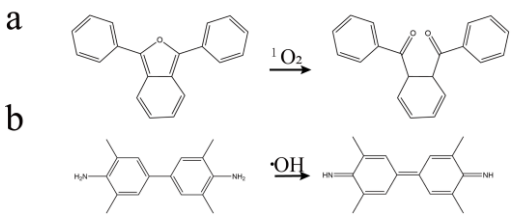

Figure S4 the reactions of DPBF and TMB.

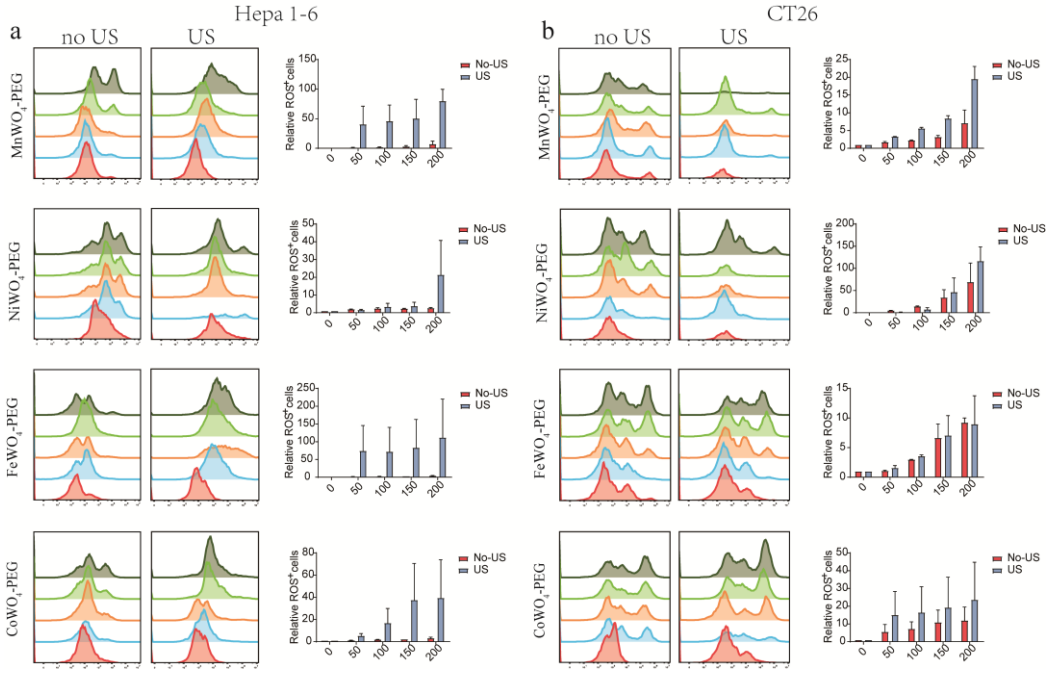

Figure S5 ROS of Hepa 1-6 (a) and CT26 (b) cells after incubation with different concentrations of MWO_4-PEG NPs in the presence or absence of US.

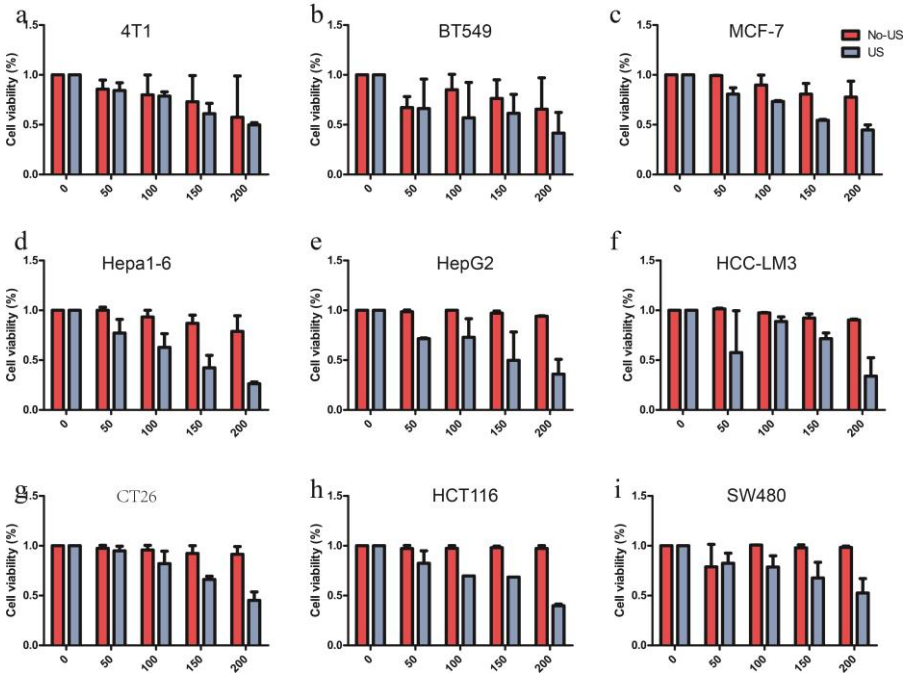

Figure S6 SDT-mediated inhibition of cell viability. The cell viability of BC, HCC and CRC were measured by Cell Counting Kit-8. The relative cell viability in the drug administration by increasing concentration of $CoWO_4$-PEG NPs (50, 100, 150, 200 μg/ml) was analyzed relatively to the untreated group (0 μg/mL). (a-c) Illustration to elucidate the decreasing cell viability of breast cancer cells, hepatocellular carcinoma cells and colorectal cancer cells treated by $CoWO_4$-PEG NPs with or without US-activation.

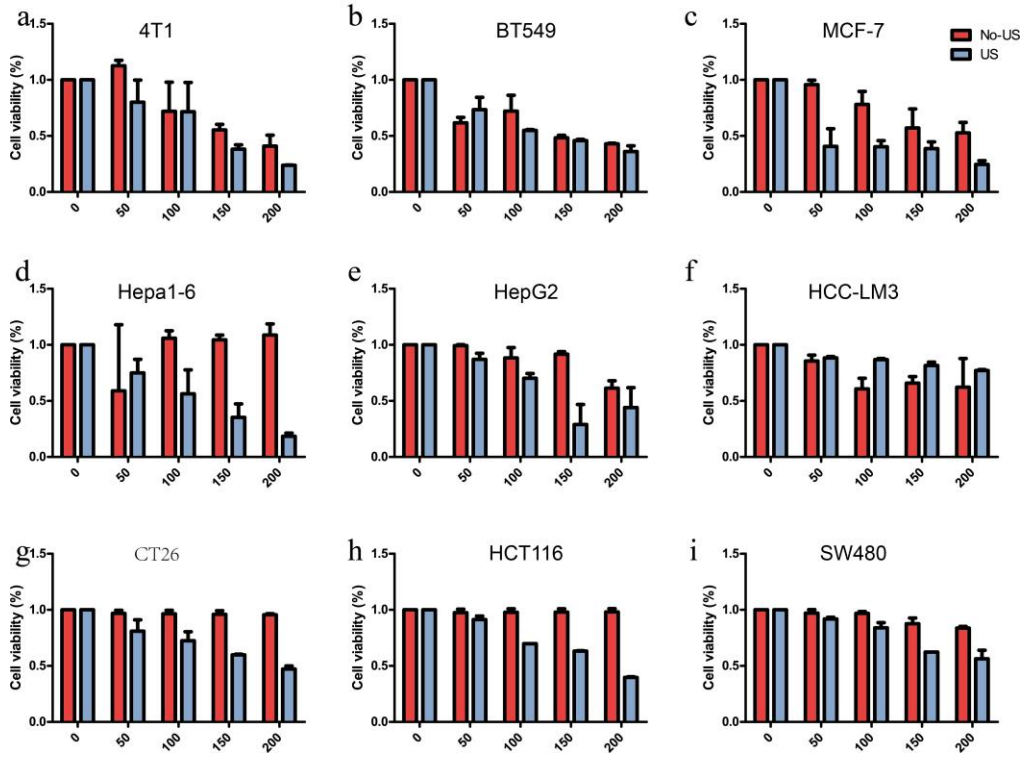

Figure S7 SDT-mediated inhibition of cell viability. The cell viability of BC, HCC and CRC were measured by Cell Counting Kit-8. The relative cell viability in the drug administration by increasing concentration of $FeWO_4$-PEG NPs (50, 100, 150, 200 μg/ml) was analyzed relatively to the untreated group (0 μg/mL). (a-c) Illustration to elucidate the decreasing cell viability of breast cancer cells, hepatocellular carcinoma cells and colorectal cancer cells treated by $FeWO_4$-PEG NPs with or without US-activation.

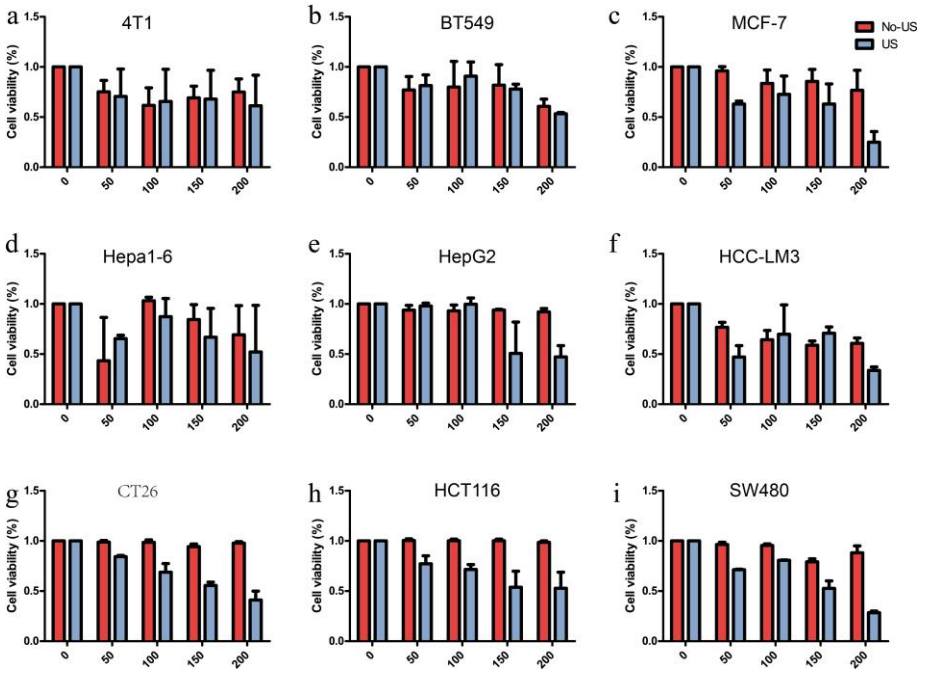

Figure S8 SDT-mediated inhibition of cell viability. The cell viability of BC, HCC and CRC were measured by Cell Counting Kit-8. The relative cell viability in the drug administration by increasing concentration of $MnWO_4$-PEG NPs (50, 100, 150, 200 μg/ml) was analyzed relatively to the untreated group (0 μg/mL). (a-c) Illustration to elucidate the decreasing cell viability of breast cancer cells, hepatocellular carcinoma cells and colorectal cancer cells treated by $MnWO_4$-PEG NPs with or without US-activation.

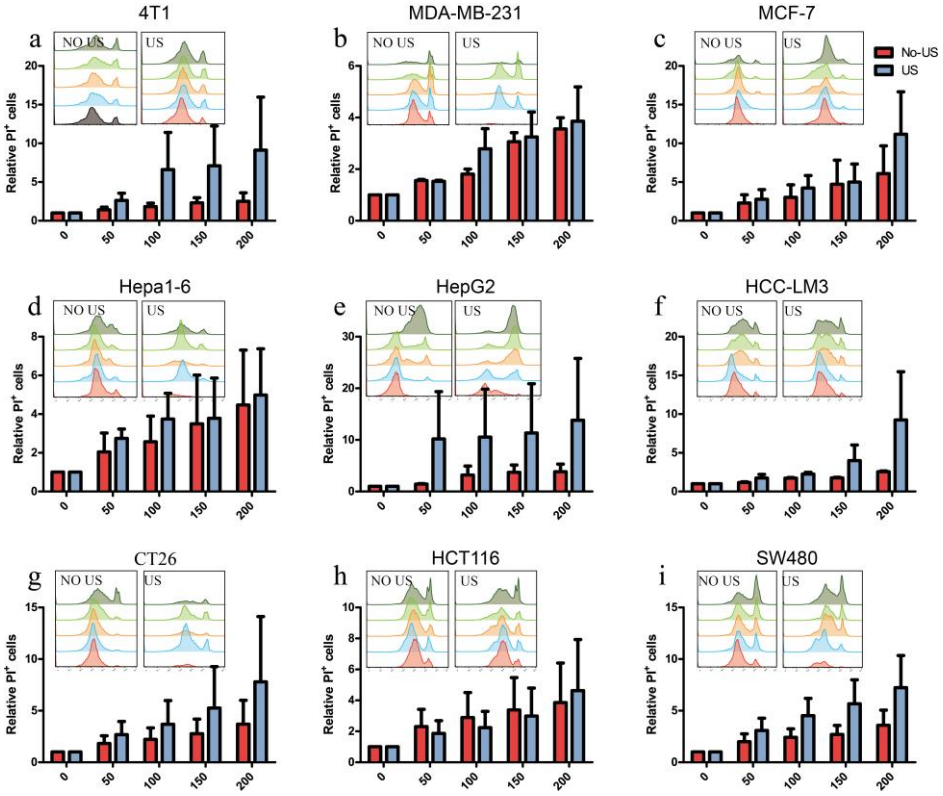

Figure S9 SDT-mediated cytotoxicity in vitro. The propidium iodide (PI) was used to stain the NPs treated BC, HCC and CRC cells to indicate apoptosis cells. The percentage of PI^+ positive cells after the administration of $CoWO_4$-PEG NPs with US activation was detected by flow cytometry. (a-c) The apoptosis rate of BC, HCC and CRC cells treated by $CoWO_4$-PEG NPs with or without US-activation.

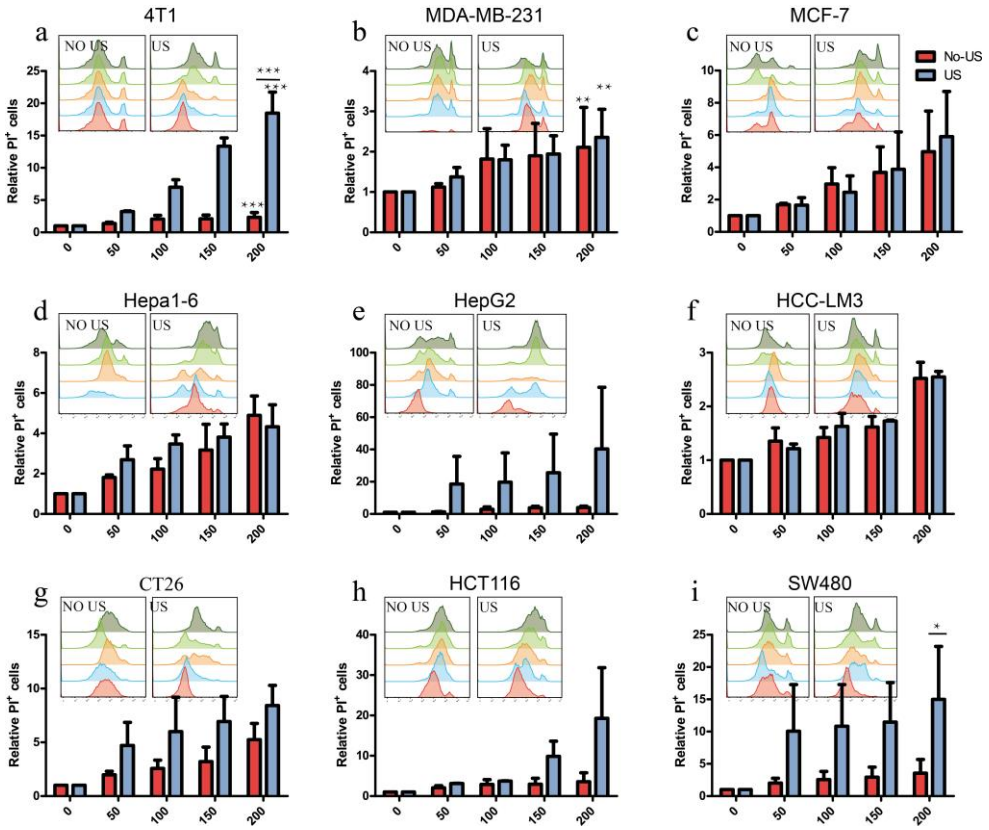

Figure S10 SDT-mediated cytotoxicity in vitro. The propidium iodide (PI) was used to stain the NPs treated BC, HCC and CRC cells to indicate apoptosis cells. The percentage of PI^+ positive cells after the administration of $FeWO_4$-PEG NPs with US activation was detected by flow cytometry. (a-c) The apoptosis rate of BC, HCC and CRC cells treated by $FeWO_4$-PEG NPs with or without US-activation.

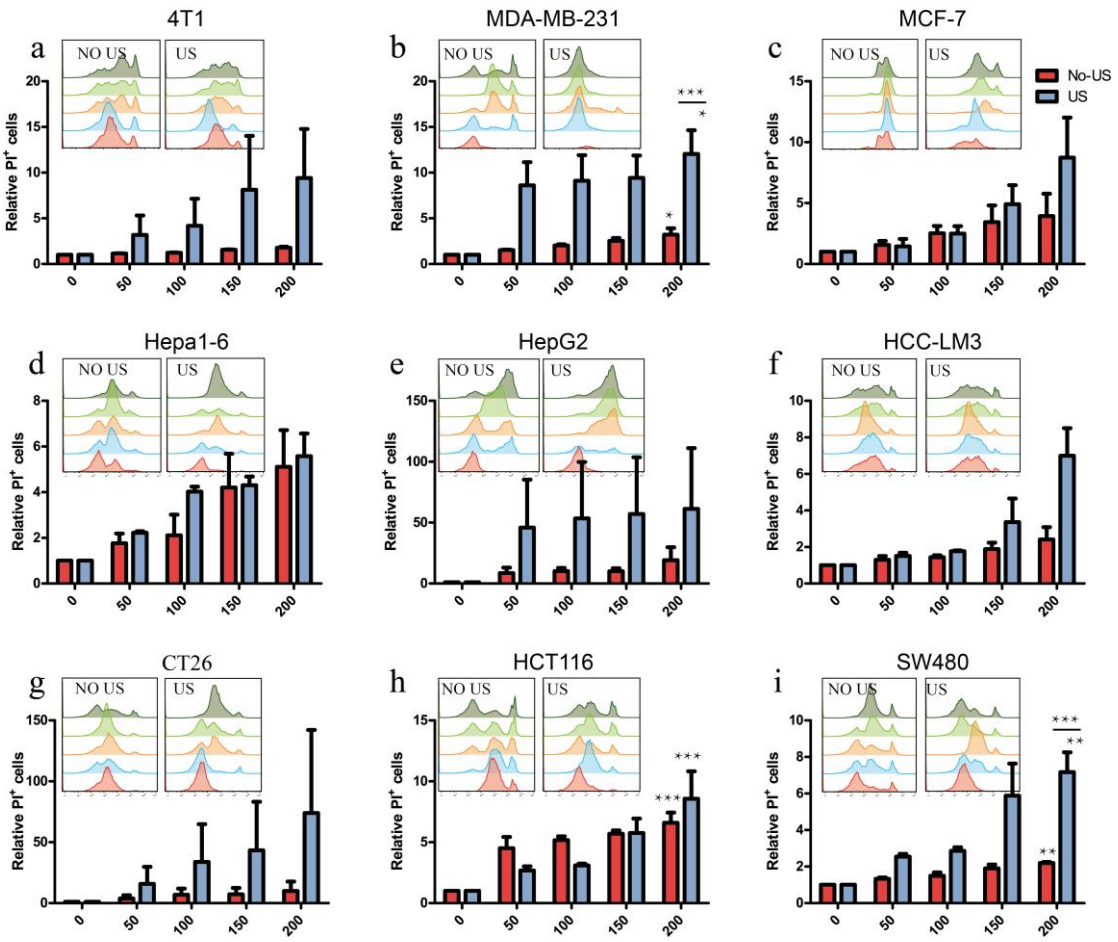

Figure S11 SDT-mediated cytotoxicity in vitro. The propidium iodide (PI) was used to stain the NPs treated BC, HCC and CRC cells to indicate apoptosis cells. The percentage of PI^+ positive cells after the administration of $MnWO_4$-PEG NPs with US activation was detected by flow cytometry. (a-c) The apoptosis rate of BC, HCC and CRC cells treated by $MnWO_4$-PEG NPs with or without US-activation.

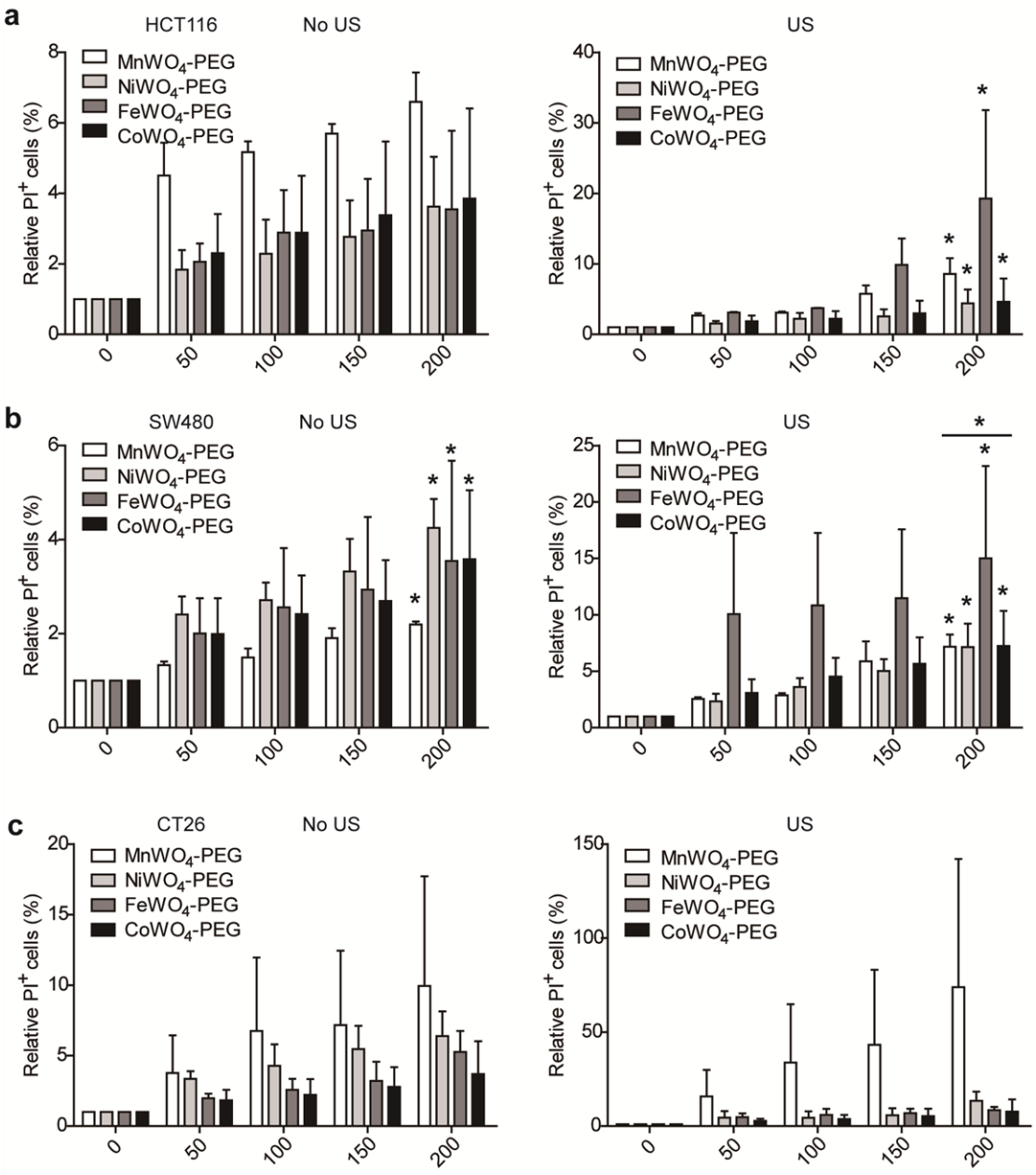

Fig. S12 SDT-mediated cytotoxicity in CRC. US triggered toxicity of MWO4-PEG NPs to cancers. The relative apoptosis rate of human BC HCT116 **(a)**, SW480 **(b)** and mouse CRC CT26 **(c)** cells treated by increasing concentration (0, 50, 100, 150, 200 μg/ml) of four MWO_4-PEG NPs (left figure) or without (right figure) US irradiation. The propidium iodide (PI) was used to stain the NPs treated CRC cells to indicate apoptosis cells. The percentage of PI^+ cells was detected by flow cytometry. Data shown are representative of 3 independent experiments. Data are represented as mean ± SD. *,** and *** represent $p < 0.05$, $p < 0.01$ and $p < 0.001$, respectively.

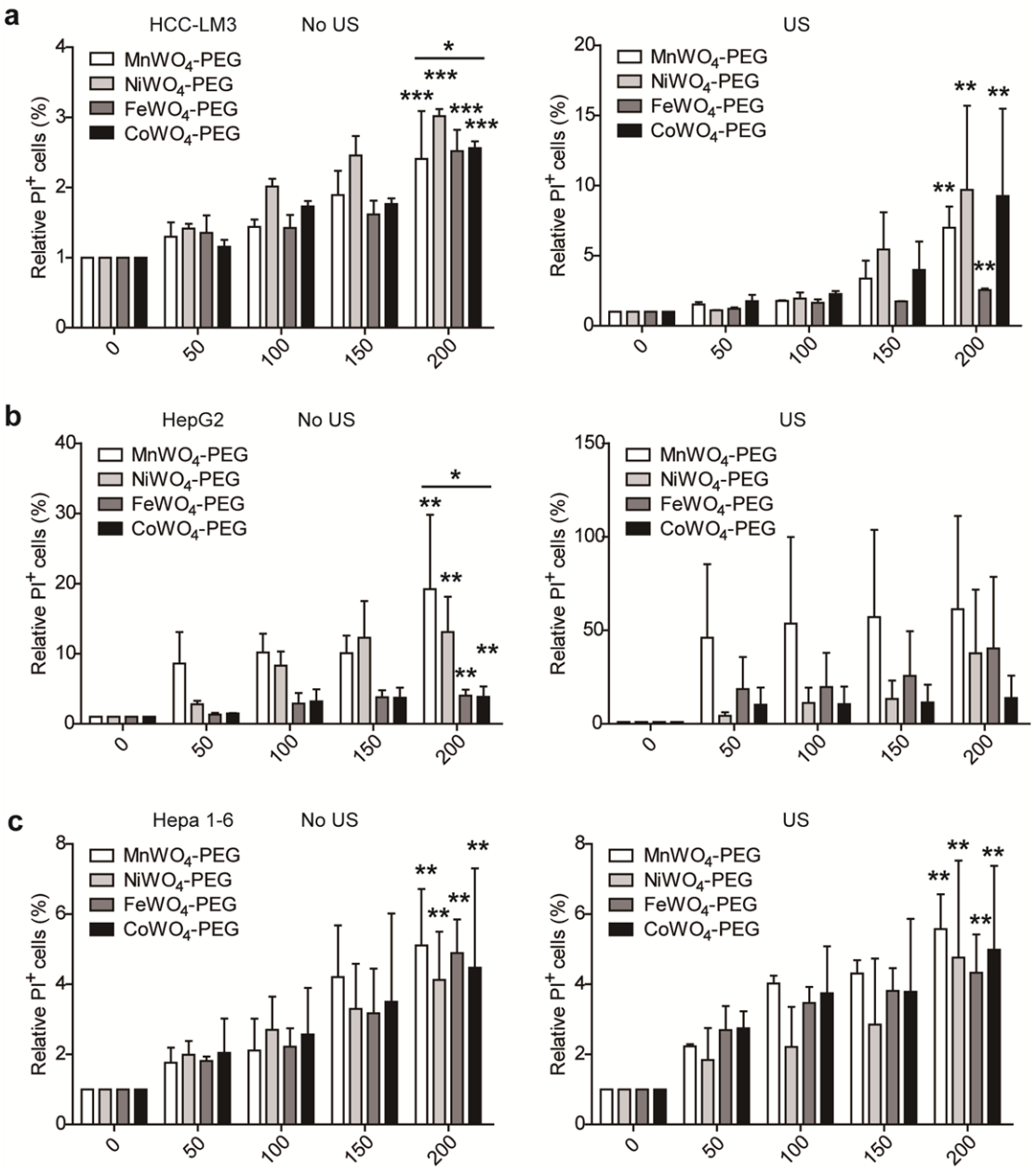

Fig. S13 SDT-mediated cytotoxicity in HCC. US triggered toxicity of MWO4-PEG NPs to cancers. The relative apoptosis rate of human HCC HCC-LM3 **(a)**, HepG2 **(b)** and mouse HCC Hepa 1-6 **(c)** cells treated by increasing concentration (0, 50, 100, 150, 200 μg/ml) of four MWO_4-PEG NPs (left figure) or without (right figure) US irradiation. The propidium iodide (PI) was used to stain the NPs treated HCC cells to indicate apoptosis cells. The percentage of PI^+ cells was detected by flow cytometry. Data shown are representative of 3 independent experiments. Data are represented as mean ± SD. *,** and *** represent $p < 0.05$, $p < 0.01$ and $p < 0.001$, respectively.